Magnesium Technology 2012
Edited by: Suveen N. Mathaudhu, Wim H. Sillekens, Neale R. Neelameggham, and Norbert Hort
TMS (The Minerals, Metals & Materials Society), 2012

MICROSTRUCTURE AND MECHANIAL PROPERTIES OF AS-EXTRUDED Mg-Sn-Al-Zn ALLOYS

Sung Hyuk Park, Young Min Kim, Chang Dong Yim, Ha-Sik Kim, Bong Sun You
Light Metals Group, Korea Institute of Materials Science, Changwon 641-831, South Korea

Keywords: Magnesium alloy, Indirect extrusion, Precipitation, Yield asymmetry

Abstract

Mg-(9-x)Sn-xAl-1Zn (x=1, 2, 3 and 4 wt.%) alloys were subjected to indirect extrusion, and the microstructure and mechanical properties of these as-extruded Mg-Sn-Al-Zn (TAZ) alloys were investigated. The TAZ alloys contain only fine Mg_2Sn second-phase particles in the α -Mg matrix, and the amount of precipitates increase with increasing Sn contents. In addition, the TAZ 811 alloy shows finer grain structure than the TAZ 541 alloy due to a larger amount of Mg_2Sn particles, which act as nucleation sites for recrystallization and/or prevention of grain growth by the pinning effect. The textures of the alloys show a typical basal pole orientation and an unusual <11-20> component in which one axis of the HCP unit cell is parallel to the extrusion axis. Tensile yield strength increases with Sn content, while ultimate tensile strength is almost identical due to the increased strain hardenability with Al content. The tension-compression yield asymmetry decreases with reducing Sn content, which is mainly due to the decrease in the amount of particles promoting twin nucleation.

Introduction

One of the major obstacles to overcome in Mg extrusions is their low extrusion speed, which is directly related to cost and energy efficiency. Normally, the extrusion speed of commercial high-strength Mg alloys, such as AZ80 and ZK60, is restricted to 0.5 to 2.5 m/min, which is well below the speeds attainable with Al alloys [1]. This is mainly due to an increase in the susceptibility to surface tearing during extrusion with increases in alloying elements, such as Al and Zn, which results from the incipient melting of second-phase particles with low melting temperatures. In regard to high-speed extrusion, it is believed that Mg–Sn-based alloys have great potential due to their higher incipient melting temperatures than conventional AZ and ZK series Mg alloys [2,3]. In addition, indirect extrusion facilitates extrusion at a higher speed than conventional direct extrusion since there is no friction between the billet and the walls of the container and therefore no friction heat can occur. In the present study, experimental Mg-(9-x)Sn-xAl-1Zn (x=1, 2, 3 and 4 wt.%) alloys were subjected to indirect extrusion, and the microstructure and mechanical properties of these as-extruded alloys were comparatively investigated.

Material and Experimental Procedures

The composition of the Mg-(9-x)Sn-xAl-1Zn (TAZ 541, 631, 721, 811) alloys used in this study are listed in Table 1. To prepare the billets for extrusion, the alloys were melted under an inert atmosphere containing a mixture of CO_2 and SF_6 and were then stabilized at 700°C and poured into a steel mould pre-heated to 200°C. After casting, the billets were homogenized under the heat treatment conditions shown in Table 1 and then water-quenched to induce a supersaturated solid solution. The billets were 80 mm in diameter and 200 mm long. Prior to indirect extrusion, the billets were pre-heated in a resistance furnace set at 250°C for 1 h. The extrusions were conducted at an initial billet temperature of 250°C and a ram speed of 1.3 mm/s (equal to the rod speed of about 2 m/min). This temperature is somewhat lower than those usually used in the conventional direct extrusion of Mg alloys. A rod profile was extruded with a fixed extrusion ratio of 25. Microstructural examinations were conducted on the midsections parallel to the extrusion direction (ED). The texture was examined using X-ray diffraction on the cross-sectional area of the extrudates. The longitudinal tensile and compressive properties of the as-extruded condition were measured at room temperature at an initial strain rate of 1.0×10^{-3} s^{-1} using round tensile specimens with a gauge diameter of 6 mm and a gauge length of 25 mm as well as cylindrical compressive specimens that were 8 mm in diameter and 12 mm in high.

Table 1. Chemical compositions (wt.%) and homogenization conditions of Mg-(9-x)Sn-xAl-1Zn alloys.

Alloy	Sn	Al	Zn	Mg	Temp. (°C)	Time (hour)
TAZ541	5.01	3.96	0.96	Bal.	460	8
TAZ631	5.95	3.01	0.97	Bal.	480	6
TAZ721	7.02	1.96	0.95	Bal.	500	4
TAZ811	7.95	0.95	0.95	Bal.	500	4

Results and Discussion

Second-phase particle

Various second-phase particles, such as Mg_2Sn, $Mg_{17}Al_{12}$, and $MgZn_2$ can be formed during extrusion by dynamic precipitation of alloying elements Sn, Al, and Zn, which are in a solid solution state before extrusion. To predict the type and amount of second-phase particles formed in extrudates, the phase diagram of the Mg-(9-x)Sn-xAl-1Zn system was calculated using the PANDAT 7 software based on the CHAPHAD with the thermodynamic database. Although the initial billet temperature and extrusion conducting temperature were 250°C, the exit temperature, which is considered to be closer to the actual temperature of alloys experienced during the extrusion process, was approximately 290°C. According to the calculated phase diagram shown in Fig. 1a, the microstructure of the as-extruded TAZ alloys used in this study consists of α -Mg and Mg_2Sn phases with no other second-phase particles irrespective of the amount of alloying element (Sn or Al), and the calculated amount of Mg_2Sn phase increases from

2.6 to 4.6 wt.% as the Sn content increases (Fig. 1b). These results coincide with the X-ray diffraction pattern results of the as-extruded TAZ alloys, which show only two types of peaks of α - Mg and Mg_2Sn even in TAZ541 alloys with a relatively large amount of 4 wt.% Al.

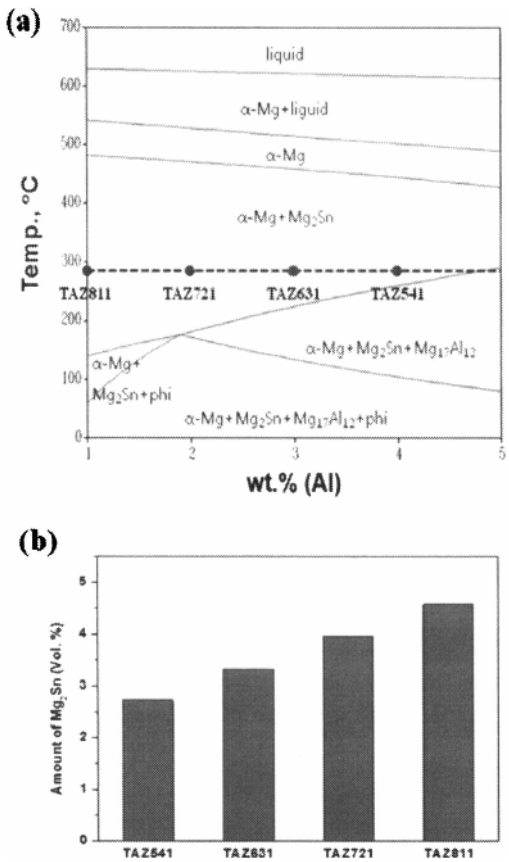

Figure 1. (a) Stable phase diagram and (b) amount of Mg_2Sn phase of TAZ alloys extruded at 290°C calculated with PANDAT software.

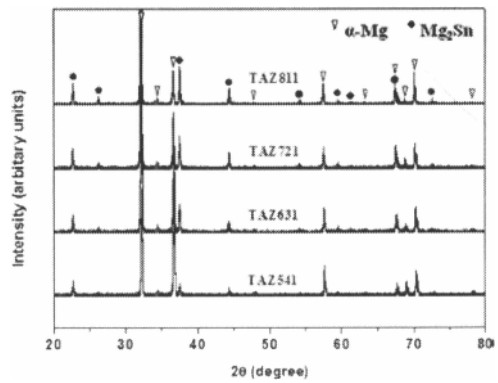

Figure 2. X-ray diffraction patterns of TAZ alloys

Microstructure

The microstructures of the as-extruded TAZ alloys are shown in Fig. 3. Coarse grains with an average size of ~300 ㎛ prior to extrusion were changed into fine grains as a consequence of dynamic recrystallization (DRX) during extrusion. The grain size of the as-extruded TAZ alloys slightly decreases with increasing Sn content. This is due to the volume fraction of fine Mg_2Sn particles that precipitate out during extrusion and act as nucleation sites for recrystallization and/or prevention of grain growth by the pinning effect. Therefore, the TAZ 811 alloy with the largest amount of precipitates shows finer grain structure (~2.2 ㎛) than the TAZ 541 alloy (~5.8 ㎛) with a relatively small amount of Mg_2Sn particles.

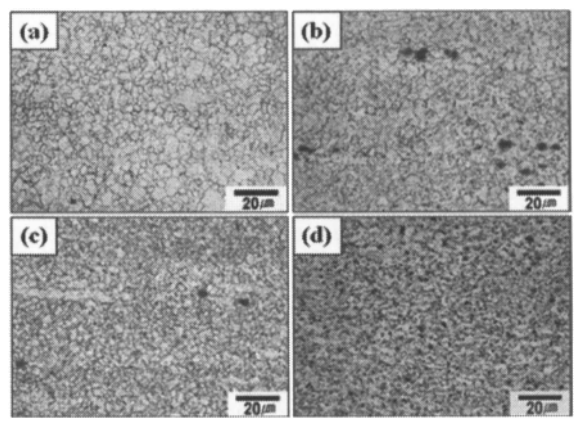

Figure 3. Optical micrographs of as-extruded (a) TAZ541, (b) TAZ631, (c) TAZ721, and (d) TAZ811 alloys

Fig. 4 shows inverse pole figures of the as-extruded TAZ alloy specimens. Most of the extruded Mg alloys have a typical extrusion texture, where the <0002> basal poles and <10-10> prismatic poles are mainly oriented perpendicular and parallel to the ED, respectively [4,5]. Although the textures of as-extruded TAZ alloys show a typical basal pole orientation, they have a strong <11-20> component in which one axis of the HCP unit cell

is parallel to the extrusion axis. Although <10-10> texture component preferentially aligned with the extrusion axis is very dominant in extruded Mg alloys, it is possible to develop other texture components by controlling the chemical composition and deformation temperature. For example, AZ31 Mg alloy indirectly extruded at 250°C shows ring type texture in which prismatic poles are randomly oriented without preferred orientation [6]. On the other hand, a double texture component with <10-10>+<11-20> is developed in Mg-Mn alloy extruded at 300°C [7], and some RE additions generate a <11-21> peak [7,8]. Therefore, <11-20> texture of TAZ alloys is attributed to the addition of Sn, which may affect the activation of slip systems or temperature during extrusion. As the Schmid factor values of slip systems and/or twin variants activated during the deformation depend on not only basal pole orientation but also prismatic pole orientation, these prismatic texture components play an important role in deformation behavior [9-11]. Therefore, further research on the DRX mechanism of TAZ alloys is required to understand the relationship between the chemical composition and texture developed during extrusion.

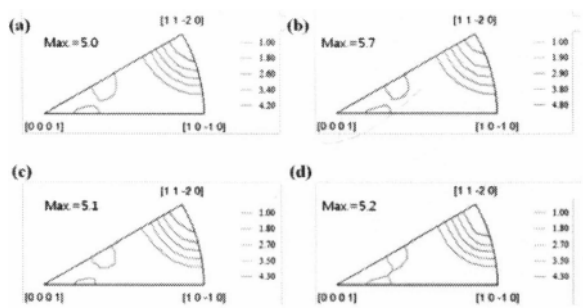

Figure 4. Inverse pole figures of (a) TAZ541, (b) TAZ631, (c) TAZ721, and (d) TAZ811 alloys with respect to the extrusion direction.

Mechanical properties

The results of the tensile tests are summarized in Table 2. As the grain size decreases and the amount of precipitates increases with increasing Sn content, the TAZ alloys with high Sn content show higher yield strength due to the combined effects of grain boundary hardening and precipitation hardening. While strain hardenability increases with Al content (Table 2), so that the TAZ alloys with low Sn content exhibit nearly identical tensile strength with those having high Sn content in spite of their low yield strength.

Fig. 5 shows the tensile and compressive yield stresses and tension-compression yield asymmetry, CYS/TYS. Because a decrease in grain size enhances the activation stress of slip and twinning, both tensile and compressive yield strengths increase with Sn content. However, precipitate particles promote {10-12} twin nucleation as the Orowan stress on twinning dislocations leads to an increase in stress around particles [12]. Accordingly, although an increase of particles causes an increase in tensile yield strength by precipitation hardening, compressive yield strength decreases with an increasing amount of particles due to the reduction of twinning stress, which is activation stress driving twin nucleation. For this reason, the increment of tensile yield strength with Sn content is slightly larger than that of compressive yield strength, resulting in a decrease of yield asymmetry with decreasing Sn content as shown in Fig. 5.

Table 2. Tensile properties of as-extruded TAZ alloys.

Alloy	YS (MPa)	UTS (MPa)	EL (%)	n
TAZ541	217	340	19.6	0.24
TAZ631	238	332	18.5	0.20
TAZ721	261	342	16.6	0.17
TAZ811	265	333	17.7	0.15

* YS, UTS, EL and n represent the 0.2 % offset yield strength, ultimate tensile strength, elongation, and work hardening exponent, respectively.

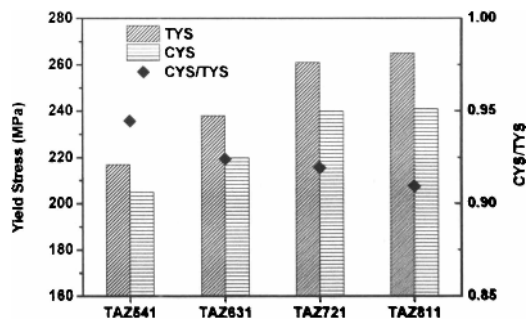

Figure 5. Tensile and compressive yield stresses and CYS/TYS

Conclusions

Mg-(9-x)Sn-xAl-1Zn (x=1, 2, 3 and 4 wt.%) alloys were subjected to indirect extrusion, and the microstructure and mechanical properties of these as-extruded alloys were investigated. The TAZ 811 alloy shows smaller grain size than the TAZ 541 alloy due to a larger amount of Mg_2Sn particles, which act as nucleation sites for recrystallization and/or prevention of grain growth by the pinning effect. Tensile yield strength increases with Sn content due to the combined effects of grain boundary hardening and precipitation hardening. The yield asymmetry between tension and compression reduces with decreasing Sn content, which is mainly due to the decrease in the amount of particles promoting twin nucleation.

References

1. C.J. Bettles and M.A. GibsonY, "Current wrought magnesium alloys: strengths and weaknesses" *JOM*, 57 (2005) 46-49.

2. D.H. Kang et al., "Development of creep resistant die cast Mg-Sn-Al-Si alloy" *Mater. Sci. Eng. A*, 413-414 (2005), 555-560.

3. W.L. Cheng et al., "Strength and ductility of novel Mg-8Sn-1Al-1Zn alloys extruded at different speeds," *Materials Letters*, 65 (2011) 1525-1527.

4. S. Yi, "Investigation on the deformation behavior and the texture evolution in magnesium wrought alloy AZ31", *Fakultät für Natur- und Materialwissenschaften*, Technischen Universtität Clausthal (2005).

5. J. Bohlen et al., "Microstructure and texture development during hydrostatic extrusion of magnesium alloy AZ31", *Scripta Mater.* 53 (2005) 259-264.

6. S. Mueller et al., "Microstructure and mechanical properties of the extruded Mg-alloys AZ31, AZ61, AZ80", *Int. J. Mater. Res.* 97 (2006), 1384-1391.

7. J. Bohlen et al., "Influence of the alloying additions on the microstructure development of extruded Mg-Mn alloys", *Magnesium Technology* (2009) 225-230.

8. N. Stanford and M.R. Barnett, "The origin of "rare earth" texture development in extruded Mg-based alloys and its effect on tensile ductility", *Mater. Sci. Eng. A* 496 (2008) 399-408.

9. S.H. Park et al., "Activation mode dependent {10-12} twinning characteristics in a polycrystalline magnesium alloy", *Scripta Mater.* 62 (2010) 202-205.

10. S.G. Hong et al., "Role of {10-12} twinning characteristics in the deformation behavior of a polycrystalline magnesium alloy", *Acta Mater.* 58 (2010) 5873-5885.

11. S.G. Hong et al., "Strain path dependence of {10-12} twinning activity in a polycrystalline magnesium alloy", *Scripta Mater.* 64 (2011) 145-148.

12. J.D. Robson et al., "Effect of particles in promoting twin nucleation in a Mg-5 wt.% Zn alloy", *Scrtipa Mater.* 63 (2010) 823-826.